Nanostructure-property relations for phase-change random access memory (PCRAM) line cells

Kooi, B. J.; Oosthoek, J. L. M.; Verheijen, M. A.; Kaiser, M.; Jedema, F. J.; Gravesteijn, D. J.

Published in:
Physica Status Solidi B-Basic Solid State Physics

DOI:
10.1002/pssb.201200371

Publication date:
2012

Phys. Status Solidi B **249**, No. 10, 1972–1977 (2012) / **DOI** 10.1002/pssb.201200371

Part of Special Issue
Phase-change memory: Science and applications

physica status solidi b
www.pss-b.com
basic solid state physics

Nanostructure–property relations for phase-change random access memory (PCRAM) line cells

B.J. Kooi*[,1], J.L.M. Oosthoek[1], M.A. Verheijen[2], M. Kaiser[2], F.J. Jedema[3], and D.J. Gravesteijn[3]

[1] Zernike Institute for Advanced Materials, University of Groningen, Nijenborgh4, 9747 AG Groningen, The Netherlands
[2] Philips Innovation Services, High Tech Campus 11 (WBC), 5656 AE Eindhoven, The Netherlands
[3] NXP Semiconductors, Central R&D,High Tech Campus 32, 5656 AE Eindhoven, The Netherlands

Received 15 June 2012, revised 13 August 2012, accepted 13 August 2012
Published online 13 September 2012

Dedicated to Stanford R. Ovshinsky on the occasion of his 90th birthday

Keywords electrical properties, electromigration, phase-change RAM, random access memory, transmission electron microscopy

* Corresponding author: e-mail B.J.Kooi@rug.nl, Phone: +3150363 4896, Fax: +3150363 4879

Phase-change random access memory (PCRAM) cells have been studied extensively using electrical characterization and rather limited by detailed structure characterization. The combination of these two characterization techniques has hardly been exploited and it is the focus of the present work. Particularly, for improving the reliability of PCRAM such combined studies can be considered indispensable. Here, we show results for PCRAM line cells after series of voltage pulses with increasing magnitude are applied, leading to the first minimum sized amorphous mark, maximum amorphous resistance and over-programming, respectively. Furthermore, the crucial effect of electromigration limiting the endurance (cyclability) of the cells is demonstrated.

1 Introduction Phase-change random access memory (PCRAM) technologies hold strong cards for replacing the currently popular Flash memory [1]. Even though Flash memory exceeds the expectations that were foreseen in the past, it is expected in the near future that further downscaling is no longer possible [1–3]. PCRAM on the other hand is scalable with the next generations of lithography, requires less lithographic steps, has a higher (over)writing speed, improved endurance (cyclability) and requires less program energy [1–3].

PCRAM exploits the large (three to four orders of magnitude) difference in electrical resistance of the amorphous and crystalline states of phase-change materials, which are renowned for their extremely fast crystallization kinetics at relatively high temperatures (e.g. 400 °C) and amorphous-phase stability at operating temperatures (e.g. up to 100 °C). A fast, high-energy electrical (RESET) pulse transforms the crystalline cell into an amorphous state by melt-quenching. The crystalline state can be recovered by applying a longer low-energy (SET) pulse that heats the cell optimally below the melting temperature. The higher mobility of the atoms allows crystallization of the amorphous region during the SET pulse. This can also be performed fast, within 100 ns, but not as fast as melt-quenching that can in principle be performed with sub-picoseconds pulses [4].

Despite the large potential of PCRAM still reliability issues have to be addressed, which require improved understanding of the relation between nanostructure and properties of actual PCRAM cells. A very suitable technique for establishing this relation is transmission electron microscopy (TEM). Ideally, the electrical switching and characterization are combined employing *in situ* TEM observations. Recent examples of this approach are provided in Refs. [5, 6]. However, disadvantage of this approach is that locally the PCRAM cell (i.e. the layers above and below the active phase-change medium) has to be thin in order to allow for TEM imaging. This reduced thickness clearly alters the thermal properties and thereby also the electrical properties of the PCRAM cells, i.e. the cells in a memory will not behave the same as the *in situ* analysed cells. In order to avoid these effects we performed electrical characterization on real

memory cells and brought these cells to certain well-defined final states and then prepared (locally thinned) the cells such that they could be analysed by TEM. In this way, we are able to establish and understand nanostructure-property relations for actual memory cells.

Earlier TEM studies of PCRAM cells concentrated on the most popular phase-change material $Ge_2Sb_2Te_5$ [5, 6] that can be typified as a nucleation dominant material [1]. In contrast, in the present work we analyse a so-called fast-growth type material. Thermal erasure of an amorphous mark in this type of material does not depend on nucleation, but only on (re)growth from the crystalline rim. However, during electrically driven erasure, after threshold switching, crystalline filaments are expected to play a crucial role.

2 Experimental Phase change line cells with designed dimensions $250 \times 50 \times 15\,nm^3$ were produced by e-beam lithography. The details of device fabrication can be found elsewhere [7, 8].

Before TEM samples were prepared, the line cells were electrically tested and characterized [8] and brought to known specific final electrical states, i.e. a series of PCM modules differing in their programming history (number of SET/RESET cycles or RESET current used) have been analysed. Details on the programming history will be specified in Section 3 below for each analysed cell individually. Duration of all RESET pulses was 50 ns and of the SET pulses was 250 ns, but with a 250 ns rising edge and a 400 ns falling edge. Example oscilloscope traces of used electrical pulses for (a) RESET (switching from crystalline to amorphous state), (b) SET (switching from amorphous to crystalline state) are shown in Fig. 1.

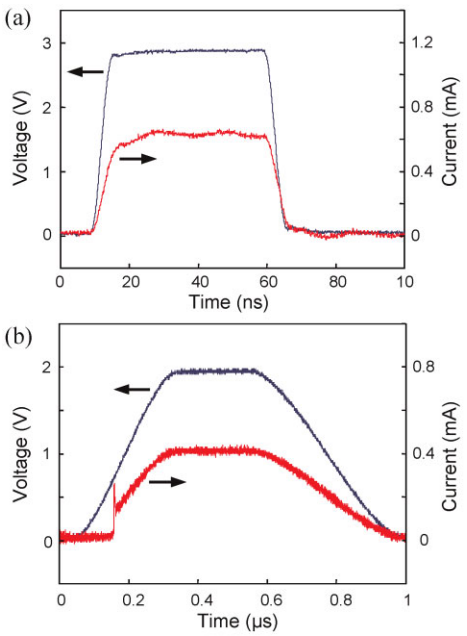

Figure 1 (online colour at: www.pss-b.com) (a) Example of 50 ns RESET pulse. (b) 250 ns SET pulse (250 ns rising and 400 ns falling edges) including threshold event.

TEM samples were prepared using two main steps: a mechanical polishing step followed by cutting and lift-out of a thin lamella using a focused ion beam (FIB) system. In brief: the polishing step is used to create a cross-sectional surface close to the feature of interest. Subsequently, FIB trenches are ion milled in the cross-section such that a lamella with dimensions of about 50 μm long, 10 μm wide and 6 μm deep with respect to the original surface is produced. This lamella is then lifted out and attached to a dedicated Mo grid giving more flexibility for subsequent precise (finally low, 100 pA current) FIB milling under various orientations to remove the substrate and covering nitride layer. Thus, a plane-view sample typically 300 nm thick containing the 15 nm PC layer sandwiched in oxide remains. In order to avoid charging and damaging of the vulnerable memory cell special precautions were necessary: Initially, after cross-section polishing and prior to FIB processing a thin Pt layer was deposited in a sputter coater and later also Pt strips were deposited on special locations of the lamella after lift out inside the FIB. In addition, layers that would become electrically isolated during the FIB milling procedure were first connected using conductive Pt lines to the larger Pt strip covering the sample, in order to avoid electrostatic discharges in the sample during the milling procedure. This step proved to be vital in order to keep the PCRAM cells intact and in their programmed state during the FIB sample preparation procedure. TEM studies were performed using a TECNAI F30ST TEM operating at 300 kV.

3 Results and discussion

3.1 First amorphization Although the phase-change material is amorphous after sputtering, it crystallizes during the bake-out step of the HSQ hard mask [7]. Therefore, the phase-change material in the as-produced line cells is always fully crystalline, i.e. in the SET state. In order to switch to the RESET state, an amorphous mark has to be introduced by melting the line by a voltage pulse. If the line is able to solidify sufficiently fast (in the order of nano-seconds) the molten region is quenched into the amorphous state. In order to find the minimum required voltage/current for the RESET pulse the pulse values are increased in relatively small incremental steps. A specific example for the line cells with designed dimensions $250 \times 50 \times 15\,nm^3$ is presented in Table 1 and Fig. 2, where Table 1 shows electrical results and Fig. 2 the corresponding TEM image after the final electrical pulse used. The TEM image shows that the actual dimensions of the line cell, $222 \times 58 \times 15\,nm^3$, differ from the designed ones. The electrical results show that we start melting the phase-change material for a voltage/current that is in-between 2.52 and 2.62 V or 0.560 and 0.576 mA, respectively. The initial SET resistance of the cell is 1.07 kΩ. A 3.3 kΩ series resistance is always present that functions as the transistor in an actual memory. Therefore, the actual cell voltages are lower than the values given here. The minimum RESET resistance found after the 2.62 V/0.576 mA pulse used is 426 kΩ, i.e. an increase of about 400 times.

Table 1 Resistance versus stepwise increase of RESET pulse voltage and current leading to first minimum sized amorphous mark after pulse 9.

pulse number	RESET voltage (V)	RESET current (mA)	resistance (Ω)
1	1.88	0.432	1067
2	1.96	0.448	1063
3	2.04	0.464	1065
4	2.16	0.480	1063
5	2.24	0.496	1063
6	2.34	0.536	1058
7	2.44	0.536	1061
8	2.52	0.560	1080
9	2.62	0.576	426,252

The location and size of the amorphous mark can be identified in the TEM image, where by tilting of the specimen in the TEM the contrast between the phases can be increased: Depending on tilt, crystals show relatively large variation in contrast (from light grey to black), whereas the amorphous mark does not show such changes. The approximate positions of the amorphous-crystalline boundaries detected in this way are indicated in the inset of Fig. 2. The length of the amorphous mark is 38 ± 7 nm. The amorphous mark has an hour-glass shape. This shape cannot have been developed fully during the melt-quenching process, but indicates that before the RESET pulse was applied a kind of constriction (local reduced width) was present in the line. A higher current density will of course be present in such a constricted region during the electrical pulse, which explains the position of the amorphous mark.

The reason for the presence of this type of constrictions is relatively straightforward. Initially the phase-change material film is deposited amorphous. Then during further processing high temperatures are reached (350–400 °C) and crystallites are formed. Since the phase-change material type can be classified as a so-called fast-growth material, i.e. with low nucleation rates, large crystals are formed. During formation of these large crystals in the small width of the line in a cell, the edges of the line change from straight to a more jagged pattern. On some locations, the jagged patterns of both edges of the line then lead to constrictions. These results indicate that the relatively coarse-grained nature of the phase-change material can promote constrictions, which after typically 10^6 cycles can cause failure as we will show in Section 3.4 below.

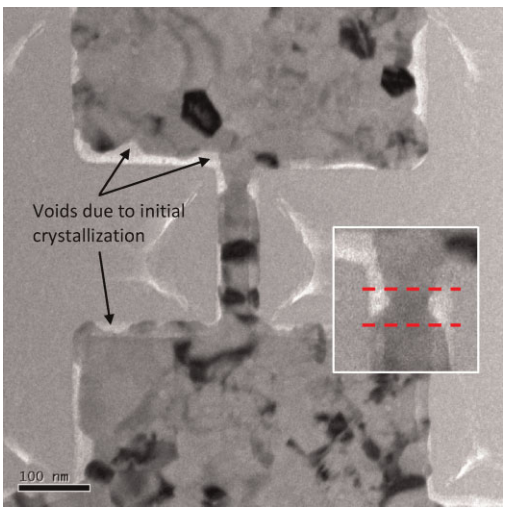

Figure 2 (online colour at: www.pss-b.com) Bright-field TEM image indicating position and size of minimum amorphous mark after pulse 9.

The minimum width in the constricted region as determined from the TEM image is 30 ± 5 nm. With a thickness of 15 nm, this means that the cross-section area is 450 nm^2. The critical current density for melting is thus $576/450 = 1.3 \pm 0.1$ A per square μm (or μA per square nm). The energy required to melt the phase-change material in this cell is $I^2Rt \approx 18$ pJ.

3.2 Increasing amorphous mark size Figure 3 shows results for the same type of line cell as described in the previous section (Table 1, Fig. 2), but now the RESET voltage/current is increased clearly beyond the critical value needed to initiate the minimum amorphous mark. The critical current for RESET is now 0.72 mA, clearly higher than the 0.57 mA found for the sample in Table 1. However, this largely scales with the cross-section area, because the line in Fig. 3 is less constricted than in Fig. 2. The critical current density for RESET as derived from Fig. 3 is $720/585 = 1.23 \pm 0.05$ A μm^{-2} (similar to that found in the previous section). The energy required to melt the phase-change material is $I^2Rt \approx 36$ pJ, twice as high as in the previous section. However, the resistance reached with this energy pulse is 2.0 MΩ, 4–5 times higher than in the previous section and correspondingly the molten region and thus the amorphous mark is clearly larger than in the previous section.

When increasing the current from 0.72 to 0.91 mA, the length of the amorphous mark is increased to nearly the full length of the line, 200 ± 10 nm and the resistance increased from 2.0 to 21.5 MΩ. So, note that the final amorphous resistance is 50 times higher for the line cell in Fig. 3 than the one in Fig. 2. The amorphous mark is only about a factor of 5 longer. This shows that there is not a direct relation between amorphous mark length and resistance of the line cell and apparently the resistivity of the amorphous material is changed an order of magnitude.

Figure 3a shows that the final RESET resistance is thus four orders of magnitude higher than the SET resistance. This demonstrates the excellent contrast between the two states of the memory.

The evolution of measured threshold voltage with amorphous resistance is shown in Fig. 3c. A linear relation holds between the two entities. For the amorphous mark shown in Fig. 3b, it would be interesting to know the threshold voltage. Unfortunately, this knowledge is not available, because after the mark was produced the cell was directly prepared for TEM imaging and a SET pulse allowing

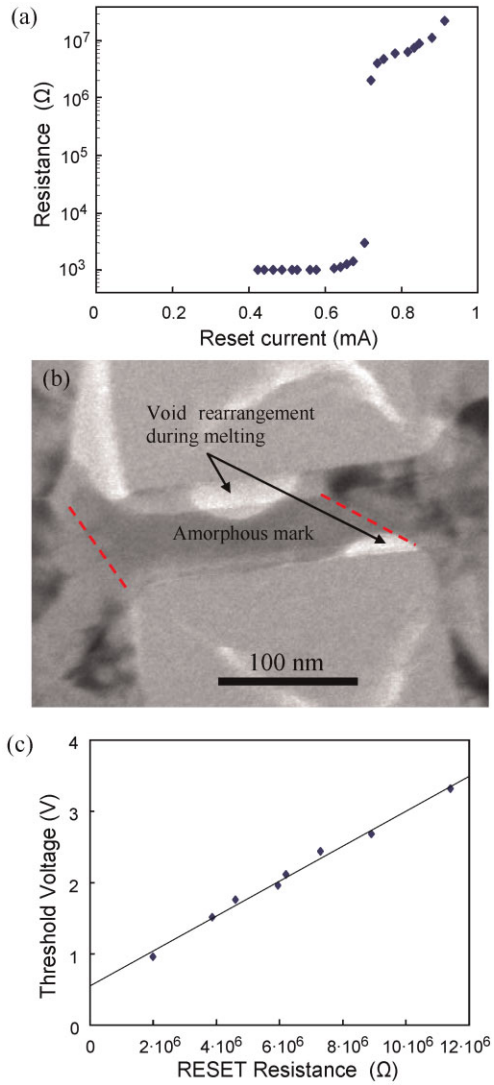

Figure 3 (online colour at: www.pss-b.com) Results for increasing the amorphous mark size to about the whole length of line cell. (a) Resistance versus stepwise increase of current during RESET pulse. (b) TEM image indicating the amorphous mark. (c) Required threshold voltage to switch amorphous mark with stepwise increasing RESET resistances.

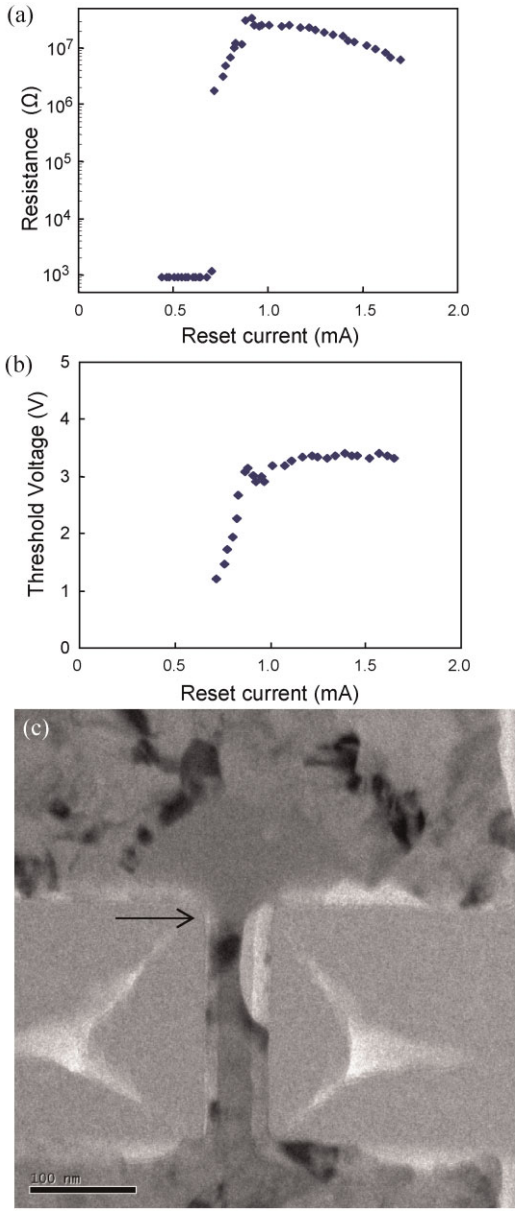

Figure 4 (online colour at: www.pss-b.com) Over-programming. (a) Resistance versus stepwise increasing RESET current. (b) Threshold voltage versus RESET current used to create amorphous mark. (c) TEM image indicating that the amorphous mark shifted out of the line into the flap.

determination of the threshold voltage was of course not applied, because this would have led to erasure of the amorphous mark. However, knowledge of the linear relation between amorphous resistance and threshold voltage allows extrapolation to the known resistance for the RESET state. Therefore, it is possible to predict a threshold voltage of 5.8 V for the mark in Fig. 3b. Using the length of the mark, the more interesting material-specific threshold field is therefore 29($\pm$5) V μm^{-1}. The accuracy is low because of the extensive extrapolation.

3.3 Over-programming If, compared to the final result of the previous section, still higher RESET currents/voltages are used, interesting behaviour is observed. The amorphous resistance reaches a maximum and is then decreasing; see Fig. 4a. This behaviour we observed earlier for similar cells as presented in Ref. [8]. In contrast, the threshold voltage also reaches a maximum, but then remains fairly constant; see Fig. 4b. In our earlier work, we even observed a still slightly increasing threshold voltage when the amorphous resistance decreases. Generally, it is assumed that a linear relation holds between threshold voltage and the amorphous state resistance (see also Fig. 3c). Such a relation holds before the maximum in resistance and threshold voltage is reached, but is not maintained for higher RESET

currents. Therefore, it is interesting to relate this so-called over-programing behaviour at high RESET currents to the structure of the line cell as observed with TEM.

Figure 4c shows TEM images of an over-programmed line cell. It is directly evident that the amorphous mark has been shifted outside the line into the phase-change flap. Since the flap does not restrict the width of the amorphous mark as the line is doing, the mark develops a mushroom shape with a dome inside the flap. Note that it is a 2D mushroom and not a 3D mushroom shape that occurs in the Ovonics-type phase-change memory [1, 2].

An important question is how deep the 'stem' of the mushroom is still inside the line of the line cell, i.e. what is the location of the crystalline-amorphous boundary in the line. For that, tilting the sample inside the TEM is very useful, indicating that the amorphous mark hardly extends into the line with the boundary only about 20 nm away from the end of the line. The length of the mark is 125 ± 7 nm. The corresponding threshold voltage for this over-programmed mark is 3.3 V. The more relevant material specific parameter is the threshold field, which is thus $26 \pm 2\ \mathrm{V\ \mu m^{-1}}$, which is actually close to the crude approximation $29 \pm 5\ \mathrm{V\ \mu m^{-1}}$ made in the previous section.

An interesting question is why the amorphous mark shifts outside the line into the flap. However, even before the mark shifts outside the line, it will in a line with uniform width (and thickness) not be located in the middle of the length of the line, but shifted towards one side [9]. The reason for this shift is the thermoelectric Thomson(-Seebeck) effect. Depending on the majority charge carrier, this asymmetric shift will occur towards the anode for p-type conduction and to the cathode for n-type conduction. For the phase-change cells, the Seebeck effect is associated with p-type conduction. Details of the observations and explanation of the asymmetric location of the amorphous mark in line cells are given in Ref. [9].

If the power of the electrical pulse is increased beyond the one needed to produce an amorphous mark up to the end of the line, it will also start melting material in the flap. During cooling particularly the region in the line that is surrounded by poorly heat-conducting SiO_x can experience too slow cooling rates and can thus recrystallize. This probably explains why the 'stem' of the amorphous mark in the line is so short. A direct relation between threshold voltage and amorphous resistance implies that they are both governed by the length of the amorphous mark. If due to over-programming, the amorphous mark moves outside the line, the shortest length l across the amorphous mark that bridges the two electrodes still determines the threshold voltage. However, the amorphous resistance R_a decreases, because the width of the current path w increases and therefore – considering for the phase-change material a constant film thickness t and resistivity ρ- the resistance R_a will decrease, because $R_a = \rho l/wt$. This explains the observed relations between threshold voltage and amorphous resistance before and after over-programming.

For actual operation, this over-programming is not desired, because it is associated with unnecessary power consumption. If the polarity of the applied electrical pulses remains the same, always the same side of the line is molten. The repeated melting during cycling will eventually lead to decomposition of the phase-change material. Sufficiently severe decomposition can then be associated with the SET stuck typically observed for line cells after 1–100 million cycles [3, 8]. An interesting point is now that if due to the Thomson(-Seebeck) effect the amorphous mark is continuously on one side of the line, the SET stuck can be avoided by starting to apply the opposite polarity of the electrical pulses. Then, the amorphous mark is shifted to the other side of the line that did not experience melting and thus decomposition up to that time. Interestingly, this strategy only works for line cells and not for the mushroom-type Ovonic cells.

3.4 Electromigration Apart from decomposition also electromigration will generally occur in the line cell, because of the repeating high current density pulses flowing through the line. In particular, lines which contain severe constrictions like depicted in Fig. 2, will be most prone to decomposition and electromigration. Figure 5 shows results

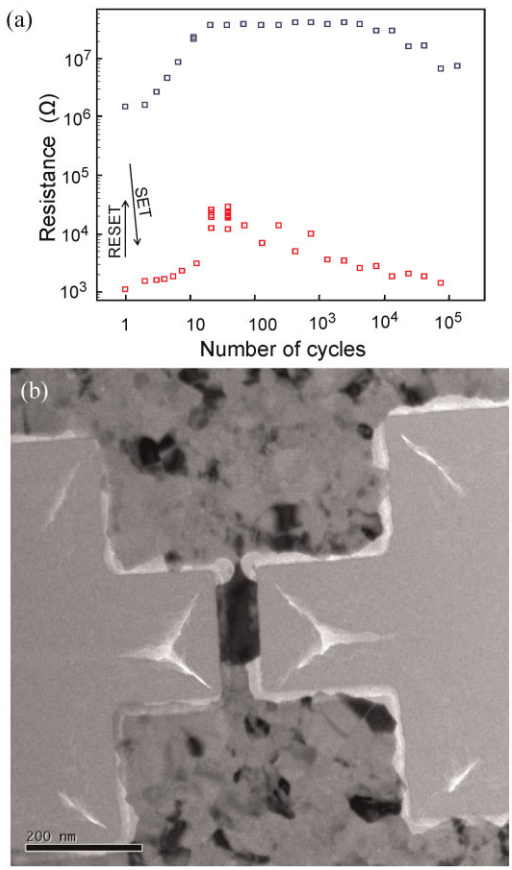

Figure 5 (online colour at: www.pss-b.com) Unusual line cell with limited number of switching cycles (1.4×10^5) due to electromigration within a constriction. (a) SET and RESET resistances as a function of switching cycles. (b) TEM image indicating that the line cell is almost broken due to electromigration, which before breakage can lead to insufficient quenching rates and thus to SET stuck.

of a line cell that is approaching its end of life after a number of switching cycles (1.4×10^5) that is much lower than average (10^7). The evolution of SET and RESET resistance with the number of switching cycles is shown in Fig. 5a. Again the excellent resistance contrast between the SET-RESET states of four orders of magnitude is shown. Already after about 10^4 switching cycles the amorphous resistance starts to decrease significantly, which is a clear indication that the cell is deteriorating due to decomposition of the phase-change material due to the repeated local melting of the phase-change material in conjunction with large electrical fields present within the molten mark [8].

The reason for the strongly reduced cyclability of the line cell can be readily deduced from the TEM image shown in Fig. 5b. Indeed, a severe constriction is present that can be associated with locally very high current densities and thus strongly accelerated decomposition and electromigration. The strong acceleration is obvious, because once a constriction is present, for instance as shown in Fig. 2, electromigration will locally reduce the width of the constriction and thereby continuously accelerate the electromigration.

Before FIB preparation the line cell was in the RESET state having a resistance of 7.3 MΩ. However, an amorphous mark cannot be detected in TEM images of this line cell taken at various tilts and it is almost certainly absent. Apparently, during TEM sample preparation crystallization has occurred. A relatively large single crystal occupies most of the total volume of the line cell up to the constriction that is present at the end of the line. The origin of this large single crystal is probably crystal growth from the melt. Due to the constriction the molten region cannot readily conduct heat along the line and the lower cooling rates then (because the phase-change material is a poor glass former) lead to growth of the large crystal. A similar argument was used to explain why most of the line was crystalline in the example shown in the previous section on over-programming.

During the voltage pulses applied to the line cells, a current density of typically $10^8\,A\,cm^{-2}$ holds in our cells; this is also the minimum value required to melt the phase-change material. In Ref. [10], a current density of $10^6\,A\,cm^{-2}$ was sufficient to melt much larger sized $Ge_2Sb_2Te_5$ lines and when this current density was continuously maintained during a few milliseconds breakage of the line due to electromigration occurred. Typical current density values for electromigration are indeed $10^6 - 10^7\,A\,cm^{-2}$ for Al or Cu metallization lines and can be even as low as $10^4\,A\,cm^{-2}$ for solder joints [11]. Therefore, it is remarkable that the line cells can still be switched typically 10^7 times with our high current densities of $10^8\,A\,cm^{-2}$. Crucial for this large number of switching cycles is the short pulses used and in addition probably the low density of grain boundaries present. Indeed, when care is taken to apply short RESET pulses like 10 ns, it is possible to reproducibly achieve for similar cells 10^9 cycles [12].

4 Conclusions The present work, demonstrates the importance of being able to correlate electrical results of phase-change cells with TEM imaging of the actual structure of the cells. Minimum amorphous mark, optimum and over-programmed amorphous marks and cell near to failure by electromigration have been imaged in conjunction with their corresponding electrical behaviour.

Particularly, the over-programming effect where the amorphous mark moves due to the Thomson effect outside the line into the phase-change flap has not been presented before and leads to special electrical behaviour where the amorphous resistance is decreasing, but the threshold voltage is remaining constant or even slightly increasing.

An important conclusion from the present work on line cells is that in case the average crystal size of the phase-change material is about equal to the width of the line cell, the edges of the line cell can become rough and can obtain jagged shapes which strongly increase the probability that locally within the line constrictions occur. Constrictions limit the lifetime of the line cell due to electric-field induced and accelerated decomposition and electromigration. Nevertheless, with similar type of cells a reproducible endurance of 10^9 cycles can still be achieved.

Acknowledgements The research was carried out under project number MC3.05241 of the Materials innovation institute M2i. Financial support from the M2i is gratefully acknowledged.

References

[1] S. Raoux, Annu. Rev. Mater. Res. **39**, 25 (2009).
[2] S. Hudgens and B. Johnson, MRS Bull. **29**, 829 (2004).
[3] M. H. R. Lankhorst, B. Ketelaars, and R. A. M. Wolters, Nat. Mater. **4**, 347 (2005).
[4] T. Ohta, N. Yamada, H. Yamamoto, T. Mitsuyu, T. Kozaki, J. Qiu, and K. Hirao, Mater. Res. Soc. Symp. Proc. **674**, V1. 1. 1 (2001).
[5] S. Meister, S.-B. Kim, J. J. Cha, H.-S. P. Wong, and Y. Cui, ACS Nano **5**, 2742 (2011); S. Meister, D. T. Schoen, M. A. Topinka, A. M. Minor, Y. Cui, Nano Lett. **8**, 4562 (2008).
[6] S.-H. Lee, Y. Jung, and R. Agarwal, Nano Lett. **8**, 3303 (2008); Y. Jung, S.-W. Nam, R. Agarwal, Nano Lett. **11**, 1364 (2011).
[7] F. J. Jedema, M. A. A. in 't Zandt, and W. S. M. M. Ketelaars, Appl. Phys. Lett. **91**, 203509 (2007).
[8] J. L. M. Oosthoek, K. Attenborough, G. A. M. Hurkx, F. J. Jedema, D. J. Gravesteijn, and B. J. Kooi, J. Appl. Phys. **110**, 024505 (2011).
[9] D. T. Castro, L. Goux, G. A. M. Hurkx, K. Attenborough, R. Delhougne, J. Lisoni, F. J. Jedema, M. Zandt, R. A. M. Wolters, D. J. Gravesteijn, M. A. Verheijen, M. Kaiser, R. G. R. Weemaes, and D. J. Wouters, IEEE Internat. Electron Devices Meeting (Washington, DC, 2007), p. 315.
[10] T.-Y. Yang, I.-M. Park, B.-J. Kim, and Y.-C. Joo, Appl. Phys. Lett. **95**, 032104 (2009).
[11] F. Ren, J.-W. Nah, K. N. Tu, B. Xiong, L. Xu, and J. H. L. Pang, Appl. Phys. Lett. **89**, 141914 (2006).
[12] L. Goux, D. T. Castro, G. A. M. Hurkx, J. G. Lisoni, R. Delhougne, D. J. Gravesteijn, K. Attenborough, and D. J. Wouters, IEEE Trans. Electron Devices **56**, 354 (2009); IEEE Trans. Electron Devices **56**, 1499 (2009).